

# Improved Advanced Control for Fault-Tolerant Operation of a Tandem Cold Rolling Mill



## Authors

**John Pittner** (left)  
researcher, Department of Electrical and Computer Engineering, University of Pittsburgh, Pittsburgh, Pa., USA  
jrpst16@pitt.edu

**Marwan A. Simaan** (right)  
Florida 21st Century Chair and Distinguished Professor of Electrical Engineering and Computer Science, University of Central Florida, Orlando, Fla., USA  
simaan@ucf.edu

Previous work examined the usage of an advanced technique for control of a tandem cold rolling mill. This paper expands on the previous work by applying improvements to this technique as developed in subsequent work for advanced control of a tandem hot mill. This investigation has resulted in a simpler method for control of tandem cold rolling, plus other improvements such as the use of virtual rolling to realize continuity of operation in the presence of various measurement faults. Simulations at the University of Pittsburgh have shown this improved control method to be highly successful.

An important, complex, highly non-linear industrial process that involves the measurement of several process variables is the tandem rolling of cold metal strip. In the authors' previous work, they developed a new, advanced method for control of this process that realized an improvement in the quality and yield of the output.<sup>1</sup> Subsequently, in their follow-up work on advanced control for tandem hot rolling, additional improvements in this control method have been realized.<sup>2</sup> These improvements carried over quite well into improving the control of tandem cold rolling. Two significant aspects of this improved controller are the simplification and improvement of the basic control method as applied to tandem cold rolling, and the addition of a virtual rolling technique to provide robustness of the controller to certain faults occurring during operation. Such faults include the degradation of certain measurements that are crucial to ensure the quality of the process output, reduce the likelihood of equipment damage, or prevent other disruptions that can result in a major loss of production. This paper presents the results of this work that show the subsequent improvements realized in the advanced control of the tandem cold mill.

## Process Description

The tandem rolling of cold metal strip is a significant process in the manufacturing and processing of metals. In general, two types of configurations are realized for the processing of steel, i.e., the stand-alone mill and the continuous mill. In the authors' initial work as described herein, the stand-alone mill (Fig. 1) was considered as an initial effort, with the continuous mill as follow-up work. What is developed for this stand-alone configuration can be used as a basis for development of the control for other stand-alone configurations and for continuous configurations.

In the stand-alone tandem cold mill, the strip is passed through a set of (typically) five pairs of independently driven work rolls, with each work roll supported by a backup roll of larger diameter. As the strip passes through the individual pairs of work rolls, the thickness is reduced by a hydraulic ram at each mill stand, which applies compressive stress in a small region denoted as the roll bite or roll gap. For this initial study, it is taken that basic instrumentation will consist of a roll force measurement at each stand, a thickness gauge at the exit of the first and last stands, a load cell at each stand, a tensiometer between each pair of stands, and with strip

Figure 1

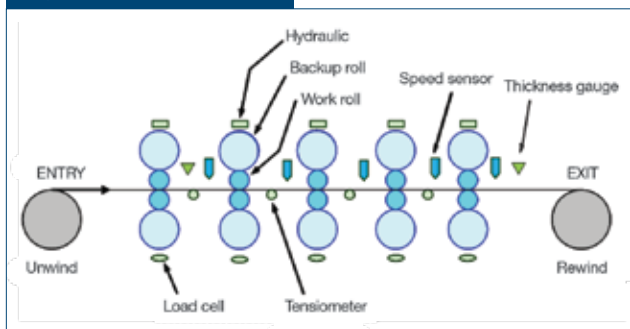
Typical stand-alone tandem cold mill.<sup>1</sup>

Table 1

Mill and Strip Parameters<sup>3</sup>

Work roll radius	11.5 inches
Mill moduli	104 tons/inch
Distance between stands	170 inches
Strip width	36 inches
Thickness ratio	1.095 (annealed/mill entry)
Young's modulus	30 x 106 lbs./inch <sup>2</sup>
Poisson's ratio	0.3
Long tons	2,240 lbs./ton

Table 2

Mill Operating Point<sup>3</sup>

Run speed, mill exit	4,000 feet/minute
Thread speed, mill exit	200 feet/minute
Mill entry thickness	0.140 inch
Exit thickness, Stand 1	0.116 inch
Exit thickness, Stand 2	0.096 inch
Exit thickness, Stand 3	0.079 inch
Exit thickness, Stand 4	0.066 inch
Exit thickness, Stand 5	0.062 inch
Tension stress, mill entry	0.0 tons/inch <sup>2</sup>
Tension stress, Stands 1,2	5.6 tons/inch <sup>2</sup>
Tension stress, Stands 2,3	5.7 tons/inch <sup>2</sup>
Tension stress, Stands 3,4	5.8 tons/inch <sup>2</sup>
Tension stress, Stands 4,5	6.0 tons/inch <sup>2</sup>
Tension stress, mill exit	1.8 tons/inch <sup>2</sup>

speed sensors, as shown in Fig. 1. In this configuration, the strip speed sensors are used for estimation of strip thicknesses using mass flow techniques. While this complement of instrumentation is taken as a basis for this initial work, the results of this investigation also are useful for other arrangements of measurements on other mills.

## Process Model

A mathematical model of the tandem cold strip rolling process consists of a set of mathematical expressions that relate the rolling parameters to each other. As a part of previous work, a model was developed based on what has been widely accepted as being suitable for control research.<sup>3</sup> The model was verified wherein simulation results were compared against data from actual installations and against the simulation results of others, with the theoretical bases also provided.<sup>3</sup> The following presents as a summary; some of the salient features of the previously developed model with more complete detail are described in Reference 3. In this investigation, an operating point was selected based on a fully threaded condition, operating between thread and run speeds, with mill and strip parameters and operating point as shown in Tables 1 and 2.

The prediction of the specific roll force in the roll bite area is:

$$P = (\bar{k} - \bar{\sigma}) \sqrt{R_p \delta} (1 + 0.4 \alpha) \quad (\text{Eq. 1})$$

where

$$\alpha = \sqrt{\frac{h_{out}}{h_{in}}} \exp\left(\frac{\mu \sqrt{R_p \delta}}{h}\right) - 1 \quad (\text{Eq. 2})$$

and where

$\bar{k}$  = the mean resistance to deformation of the material,  
 $\bar{\sigma}$  = the mean tension stress of the strip

(i.e.,  $\bar{\sigma} = \frac{\sigma_{in} + \sigma_{out}}{2}$ , where  $\sigma_{in}$  and  $\sigma_{out}$  are the

strip tension stresses at the stand input and output),  
 $\mu$  = the friction coefficient,  
 $R_p$  = the deformed work roll radius, which is estimated using the Hitchcock approximation,<sup>4</sup>

$\delta$  = the stand draft (i.e.,  $\delta = h_{in} - h_{out}$ , where  $h_{in}$  and  $h_{out}$  are the strip input and output thickness of the stand) and  
 $\bar{h}$  = the mean strip thickness.

The deformed work roll radius is estimated using the Hitchcock approximation as:

$$R_p = R \left( 1 + \frac{16(1-\nu^2)P}{\pi E \delta} \right) \quad (\text{Eq. 3})$$

where

$R$  = the undeformed work roll radius,  
 $\nu$  = Poisson's ratio and  
 $E$  = Young's modulus, which is taken as constant for this evaluation.

A linear relationship for the output thickness  $h_{out}$  is:

$$h_{out} = S + S_0 + \frac{F}{M} \quad (\text{Eq. 4})$$

where

$S$  = the position of the roll gap position actuator,  
 $S_0$  = the intercept of the linearized approximation,  
 $F$  = the total rolling force (equal to  $PW$ , where  $W$  is the strip width) and  
 $M$  = the elastic stretch of the mill stand under the application of the roll force  $F$ .

The strip speed exiting the roll bite can be estimated using the forward slip  $f$ , where  $f$  is defined as the ratio of the increase in the velocity of the exiting strip to the peripheral speed of the roll at the neutral plane, i.e.:

$$f = \frac{V_{out} - V_0}{V_0} \quad (\text{Eq. 5})$$

where  $V_{out}$  is the exit strip speed and  $V_0$  is the roll peripheral speed. A more useful relationship for control development is that of Ford, Ellis and Bland,<sup>5</sup> wherein the forward slip is expressed as:

$$f = \left( \frac{R_p}{h_{out}} \right) (\beta_n)^2 \quad (\text{Eq. 6})$$

where

$$\beta_n = \frac{\varphi_1}{2} - \frac{\delta k + \sigma_{in} h_{in} - \sigma_{out} h_{out}}{4k R_p \mu} \quad (\text{Eq. 7})$$

with

$$\varphi_1 = \left( \frac{\delta}{R_p} \right)^{1/2} \quad (\text{Eq. 8})$$

and other symbols as defined previously.

Using Young's modulus, a relationship for strip tension stress is determined as:

$$\frac{d\sigma_{i,i+1}}{dt} = \frac{E(V_{in,i+1} - V_{out,i})}{L_0}, \sigma(0) = \sigma_0 \quad (\text{Eq. 9})$$

where  $L_0$  is the distance between the centerlines of the adjacent stands, and the output and input strip speeds at the adjacent stands are  $V_{out,i}$  and  $V_{in,i+1}$ .

The controller of the position of the hydraulic cylinder that sets the work roll position at the roll bite, and the controller of the peripheral speed of the work rolls, are described as single first order lags:

$$\frac{dS}{dt} = \frac{U_S}{\tau_S} - \frac{S}{\tau_S}, S(0) = S_0 \quad (\text{Eq. 10})$$

$$\frac{dV}{dt} = \frac{U_V}{\tau_V} - \frac{V}{\tau_V}, V(0) = V_0 \quad (\text{Eq. 11})$$

where

$S$  = the cylinder position,  
 $U_S$  = the controller position reference,  
 $V$  = the roll peripheral speed,  
 $U_V$  = the controller speed reference and  
the time constants of the first order lags are represented as  $\tau_S$  and  $\tau_V$ .

The interstand time delay is the time taken for an element of strip to move between adjacent stands and is approximated as:

$$\tau_{d,i,i+1} = \frac{L_0}{V_{out,i}} \quad (\text{Eq. 12})$$

where  $V_{out,i}$  is the strip speed at the output of stand  $i$ . Using these equations, a non-linear model of the process dynamics is expressed in the following state-space form as:

$$\frac{dx}{dt} = A(x)x + Bu, x(0) = x_0 \quad (\text{Eq. 13})$$

$$y = C(x)x \quad (\text{Eq. 14})$$

where

$x \in R^n$  = a vector whose elements represent the individual state variables,

$A(x) \in R^{n \times n}$  = a state-dependent matrix,

$y \in R^p$  = a vector whose elements represent the individual output variables,

$C(x) \in R^{p \times n}$  = a state-dependent output matrix,

$u \in R^m$  = a vector whose elements represent the individual control variables and

$B \in R^{n \times m}$  = a constant matrix.

Table 3 lists the variables represented by the elements of the state, control and output vectors, where  $U$  represents a control reference, and with other symbols as noted previously. The variables represented by the elements of the state vector are derived from direct measurements so that all the states are available to the controller. The elements of the  $A(x)$ ,  $C(x)$  and  $B$  matrices are given in Reference 1.

**Table 3**

**State, Control and Output Vector Variable Assignments<sup>1</sup>**

State vector		Control vector		Output vector	
$x_1$ ( $\sigma_{12}$ )	$x_8$ ( $S_4$ )	$u_1$ ( $U_{S1}$ )	$u_6$ ( $U_{V1}$ )	$y_1$ ( $h_{out1}$ )	$y_8$ ( $\sigma_{34}$ )
$x_2$ ( $\sigma_{23}$ )	$x_9$ ( $S_5$ )	$u_2$ ( $U_{S2}$ )	$u_7$ ( $U_{V2}$ )	$y_2$ ( $h_{out2}$ )	$y_9$ ( $\sigma_{45}$ )
$x_3$ ( $\sigma_{34}$ )	$x_{10}$ ( $V_1$ )	$u_3$ ( $U_{S3}$ )	$u_8$ ( $U_{V3}$ )	$y_3$ ( $h_{out3}$ )	$y_{10}$ ( $P_1$ )
$x_4$ ( $\sigma_{45}$ )	$x_{11}$ ( $V_2$ )	$u_4$ ( $U_{S4}$ )	$u_9$ ( $U_{V4}$ )	$y_4$ ( $h_{out4}$ )	$y_{11}$ ( $P_2$ )
$x_5$ ( $S_1$ )	$x_{12}$ ( $V_3$ )	$u_5$ ( $U_{S5}$ )	$u_{10}$ ( $U_{V5}$ )	$y_5$ ( $h_{out5}$ )	$y_{12}$ ( $P_3$ )
$x_6$ ( $S_2$ )	$x_{13}$ ( $V_4$ )			$y_6$ ( $\sigma_{12}$ )	$y_{13}$ ( $P_4$ )
$x_7$ ( $S_3$ )	$x_{14}$ ( $V_5$ )			$y_7$ ( $\sigma_{23}$ )	$y_{14}$ ( $P_5$ )

## Process Controller

**Background** — In the authors' previous work, they developed a new and useful advanced technique for control of the tandem cold metal rolling process.<sup>1</sup> Subsequently, they continued their work to explore the capability of the new method to realize similar improvements in the control of tandem hot metal rolling. Their work in the tandem hot mill area resulted in similar improvements plus additional improvements that offered significant advantages. These advantages are: (1) A simplification of the application of the state-dependent Riccati equation (SDRE) technique so that an on-line solution of the algebraic Riccati equation (ARE) is not required; (2) The addition of a virtual rolling function that greatly improves control of the threading process; and (3) The use of the virtual rolling function to support fault-tolerant control to improve the availability of the mill. In the initial work, as described in this paper, the application of items 1 and 3 were considered for a fully threaded stand-alone tandem cold mill. The application of item 2 for a stand-alone tandem cold mill, and the application of these three items to a continuous tandem cold mill, will be addressed in follow-up efforts.

### Simplification in the Application of the SDRE Technique

— The SDRE technique is the basis of the design of the improved controller. This emerging technique is quite popular and has recently seen a tremendous expansion in a large variety of non-linear applications, a great many of which are in industrial areas. This popularity is mostly due to its simplicity and user-friendliness when compared to other non-linear control methods, its ability to allow physical intuition in the design process and its flexibility in the choice of design parameters. These features make it very attractive and ideal for use in tandem cold and hot metal rolling control. The following describes the improved method of simplification in applying this technique, which includes a brief overview of the basic technique with more detail available in the applicable references.<sup>2,6</sup>

The basic SDRE technique is similar to the linear quadratic regulator (LQR) method except that the coefficient matrices in the state and output equations, and in the control and state weighting matrices, are state-dependent. The plant dynamics are expressed in the form of Eqs. 13 and 14, with the optimal control problem being defined in terms of minimizing the performance index as:

$$J = \frac{1}{2} \int_0^{\infty} (x'Q(x)x + u'R(x)u)dt \quad (\text{Eq. 15})$$

with respect to the control vector  $u$ , subject to the constraint (Eq. 13), where  $Q(x) \geq 0$ ,  $R(x) > 0$ ,  $Q(x)$  and  $R(x) \in C^k$  for  $k \geq 1$ , and where  $\geq$  indicates a positive semi-definite matrix,  $>$  a positive definite matrix,  $\in C^k$  indicates that a matrix has continuous partial derivatives through order  $k$ , and  $'$  indicates the matrix or vector transpose. The performance index in Eq. 15 implies finding a control law that regulates the system to the origin. The ARE:

$$A'(x)K(x) + K(x)A(x) - K(x)BR^{-1}(x)B'K(x) + Q(x) = 0 \quad (\text{Eq. 16})$$

is then solved pointwise for  $K(x)$ , where  $R^{-1}$  indicates the inverse of the matrix  $R$ , and  $A(x)$  and  $B$  are as previously noted in Eq. 13. This results in the control law:

$$u = -S(x)x \quad (\text{Eq. 17})$$

where, for the general case,

$$S(x) = R^{-1}(x)B'K(x) \quad (\text{Eq. 18})$$

The requirement that the pair  $(A(x), B)$  be pointwise stabilizable (in a linear sense) for all  $x$  in the control space ensures that a solution to Eq. 16 exists at each point. Local asymptotic stability is ensured under somewhat mild conditions; however, in general, stability over the entire control space is confirmed by simulation.<sup>6</sup> In the application to this process, the  $B$  matrix is constant and the  $Q$  and  $R$  matrices are chosen to be diagonal with constant elements. Definitions of pointwise stabilizability and asymptotic stability are as provided in the reference.<sup>1</sup>

In the simplified method for the application of the basic SDRE technique, the improved controller has three regimes of operation: (1) the basic regime, (2) the pre-roll regime and (3) the roll regime. In the basic regime, a basis is established from which the initial settings of the controller for the full range of variations of the process are determined. An off-line simulation of a typical process operating at a typical initial operating point  $x_0$  is established. Using the process model and the initial values of the elements of  $x_0$ , the elements of  $A(x_0)$  and  $C(x_0)$  are computed. Then using physical intuition and multiple simulations, a suitable controller is obtained that includes determination of the elements of the diagonal  $Q$  and  $R$  weighting matrices and the settings of the  $PI$  gains of the trims to give a well-performing controller for both the threading and running conditions. The ARE is solved

off-line to determine a gain  $S_{BA}(x_0)$  for the control law of the inner control loop of the controller, where

$$S_{BA}(x_0) = R^{-1}B'K(x_0) \quad (\text{Eq. 19})$$

and  $K(x_0)$  is the solution of the ARE at  $x_0$ .

The pre-roll regime establishes the settings of the controller just prior to when the strip enters the mill for threading. In this regime, the model used is updated by a separate system based on data collected during recent processing, and what was established in the basic regime to determine the initial inner loop controller gain and the  $PI$  settings of the outer loop trim functions. This results in the initial setting of the controller gain of the inner loop being determined to keep the dynamic characteristics of the inner loop nearly unchanged from those of the inner loop in the basic regime. This is implemented by mathematically matching the ordinary differential equations that describe the closed-loop dynamics in the basic and pre-roll regimes to determine an initial inner loop controller gain in the pre-roll regime as:

$$S_{PR}(x_0) = B^{-L}(A_{PR}(x_0) - A_{BA}(x_0)) + S_{BA}(x_0) \quad (\text{Eq. 20})$$

where

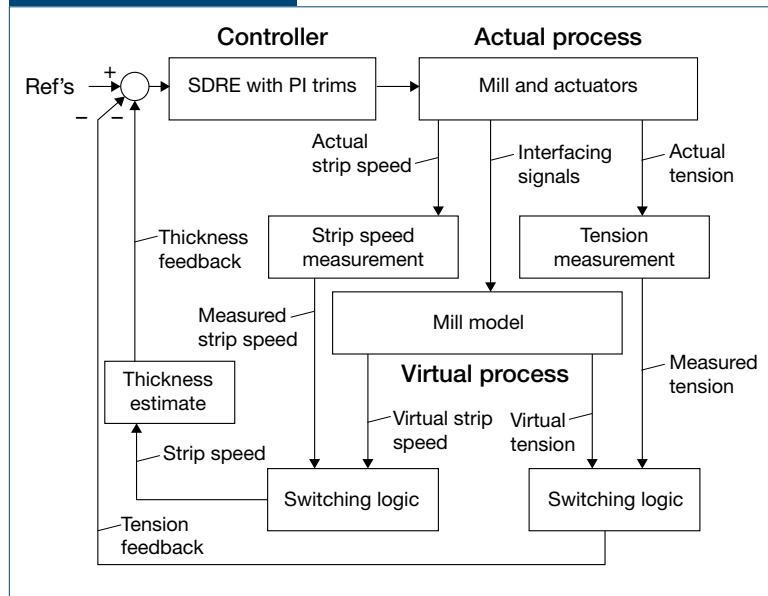
$A_{PR}(x_0)$  is determined from the updated model at the initial operating point of the pre-roll regime,  $A_{BA}(x_0)$  and  $S_{BA}(x_0)$  are as previously determined for the basic regime,  $B^{-L}$  = left inverse of the  $B$  matrix, which inverse exists and is computed as  $B^{-L} = (B'B)^{-1}B'$ , and  $A_{PR}(x_0)$ ,  $A_{BA}(x_0)$  and  $B$  correspond to the  $A$  and  $B$  matrices (Eq. 20) for the pre-roll and basic regimes.

Thus the dynamics of the inner control loop remain nearly unchanged from those of the basic regime. The gains of the  $PI$  trims are then set similarly to keep the overall outer loop characteristics very nearly unchanged from those as determined in the basic regime.

In the roll regime, the settings of the pointwise controller are adjusted at small successive instances of time, or "points," as the strip is processed through the mill. The control designer sets the time period between the successive points to provide a suitable control of the process. Thus the dynamic characteristics of the inner control loop at any given point remain reasonably close to those determined at the previous point, and to the pre-roll regime at the first point, and do not change appreciably during



Figure 3



Functional schematic of fault-tolerant control for tension and strip speed.

Eq. 24 based on Eq. 5. For initial considerations, the measurements and the model are taken to be ideal, i.e., there are no uncertainties in either. In actual practice, the model represents the process quite closely, as it is based on a wide range of data from actual installations and considerable experience, so that any deviations between the model and the real process are minor, and thus similarly between virtual tension and actual tension, and between virtual strip speed and actual strip speed.

The switching logic (Fig. 3) determines the tension feedback by switching from measured tension to virtual tension when the virtual tension is outside an acceptable operating range. Virtual tension is used since the tension measurement is less reliable as it is more susceptible to faults. The control after switching is based on virtual tension.

The velocimeters are used to provide strip speed signals from which the strip thickness at the exit of a mill stand can be determined with reduced uncertainty using the basic mass flow technique as in Eq. 23:

$$h_{out,i} = V_{in,i} h_{in,i} / V_{out,i} \quad (\text{Eq. 23})$$

where for stand  $i$  ( $i = 2, 3, 4, 5$ ),  $h_{out,i}$ ,  $h_{in,i}$ ,  $V_{out,i}$  and  $V_{in,i}$  are the thickness and strip speeds at the inputs and outputs of stand  $i$ , wherein a constant strip width through the roll gap is assumed, and with negligible dynamics through the roll gap. In this work, the strip speeds are taken to be measured by high-quality velocimeters, wherein a logic signal is usually

available to indicate a faulted speed measurement. This logic signal is used in the controller to switch to the virtual measurement of the strip speed as generated by Eq. 24. This allows the thickness estimate to be retained, although with a slightly increased uncertainty due to the uncertainty in the estimated thickness using the model.

Thus, since the tension and strip speed estimates are retained by the use of virtual rolling, the processing of the strip in the mill can continue uninterrupted with very little likelihood of a cobble, or with undesirable excursions in tension or thickness that could seriously degrade the quality of the output. However, some less-serious degradation might be expected, since the uncertainties in the virtual tension and virtual speed are greater than those in the measured values. In general, this is most likely acceptable considering the potential consequences of a faulted measurement.

More detail on the generation of the virtual speed and tension measurements is given in the following.

**Uncertainties** — To verify the overall control concept, the initial development of the control strategy is based on zero uncertainties. However, in actual applications, the uncertainties must be considered to ensure proper functioning of the controller during real scenarios. For the purposes of this initial study, the uncertainty in the tension measurement is roughly taken to be about  $\pm 2\%$  of the actual tension based on vendor data, and with some conservatism. The virtual tension is estimated to be roughly  $\pm 5\%$  of the actual tension, which is based on Eq. 9, an estimation of physical parameters, updating of the model during actual operation and experience. The acceptable unfaulty operating range of the virtual tension, considering uncertainties and to reduce the likelihood of false faults, is taken as  $\pm 10\%$  of desired tension. This translates to a range of about  $+5\%$  to  $+15\%$  in the actual tension at the upper end of the range, and about  $-5\%$  to  $-15\%$  in the actual tension at the lower end of the range. This is an overall range of about 4.85 to 6.55 tons/inch<sup>2</sup>, based on a reference of 5.7 tons/inch<sup>2</sup> in the actual tension. This range emphasizes reducing false faults with a possible slight increase in excursions in actual tension that have the potential for a slight impact on the end product. The virtual tension is used to determine a fault since it is more reliable than the tension measurement due to possible failure modes in the tension measuring system. More detail is provided in the simulations.

In the case of the velocity measurement, the uncertainty is taken to be nearly zero, which is typical for high-quality velocimeters. The uncertainty in the virtual measurement is estimated based on Eq. 5 using the following for stand 2:

$$V_{out,2,e} = (x(11)(1 + f2))k_2 \quad (\text{Eq. 24})$$

where

$V_{out,2,e}$  = the estimated virtual strip speed at the location of the velocimeter,

$x(11)$  = the linear strip speed at the neutral plane in the roll bite and

$f2$  = the forward slip.

The factor  $k_2$  allows for a reasonable approximation of the strip speed by consideration of the measured speed of the work roll drive, whatever gearing is in the work roll driveshaft, the work roll diameter and the computation of the forward slip that includes roll flattening effects in Eq. 6. During normal operation with a healthy velocimeter,  $k_2$  is calibrated by the comparison of  $V_{out,2,e}$  with the speed signal measured by the velocimeter. Thus the virtual strip speed has nearly zero uncertainty, and is recalibrated as long as the velocimeter remains healthy. The calibration is done during a single scan of the controller and only at successive points in time, with the time interval established by the designer, to ensure a high confidence in the independence of the virtual measurement should a fault occur in the velocimeter. Upon the occurrence of a fault in the velocimeter, the switch is made to the virtual speed signal, so that the period following the initial fault has nearly negligible uncertainty. It is expected that the uncertainty in this signal during extended operation beyond the period following the initial switch will remain low. This is because the uncertainty in the speed measurement in modern drives is negligible, any gearing ratio is known, any change in the roll diameter during subsequent operation is small, and any uncertainty in the slip is less significant since the slip is small compared to unity. Thus the overall uncertainty in the virtual strip speed is expected to be low during extended operation without recalibration, i.e., roughly about  $\pm 3\%$ .

It is recognized that noise will be present in both the tension measurement and the velocimeter measurement. However, in high-quality instrumentation systems, the noise in these measurements is suitably suppressed so that there is negligible noise in the actual signals at the controller.

The switching logic includes functions that reduce the likelihood of false faults. The Appendix provides more detail and gives typical examples.

**Advantages** — This novel technique provides a straightforward method of fault-tolerant control that is effective, easy to implement and user friendly. This occurs mostly due to the use of the virtual-based system in the design of the control, which also serves a dual purpose of improving the threading of the mill, which will be addressed in follow-up work, so that no additional major functions are required for fault tolerance. Further, in this method, a broad range of faults can be handled without much complexity, and the process can continue without interruption with only a minor effect on product quality.

## Simulations

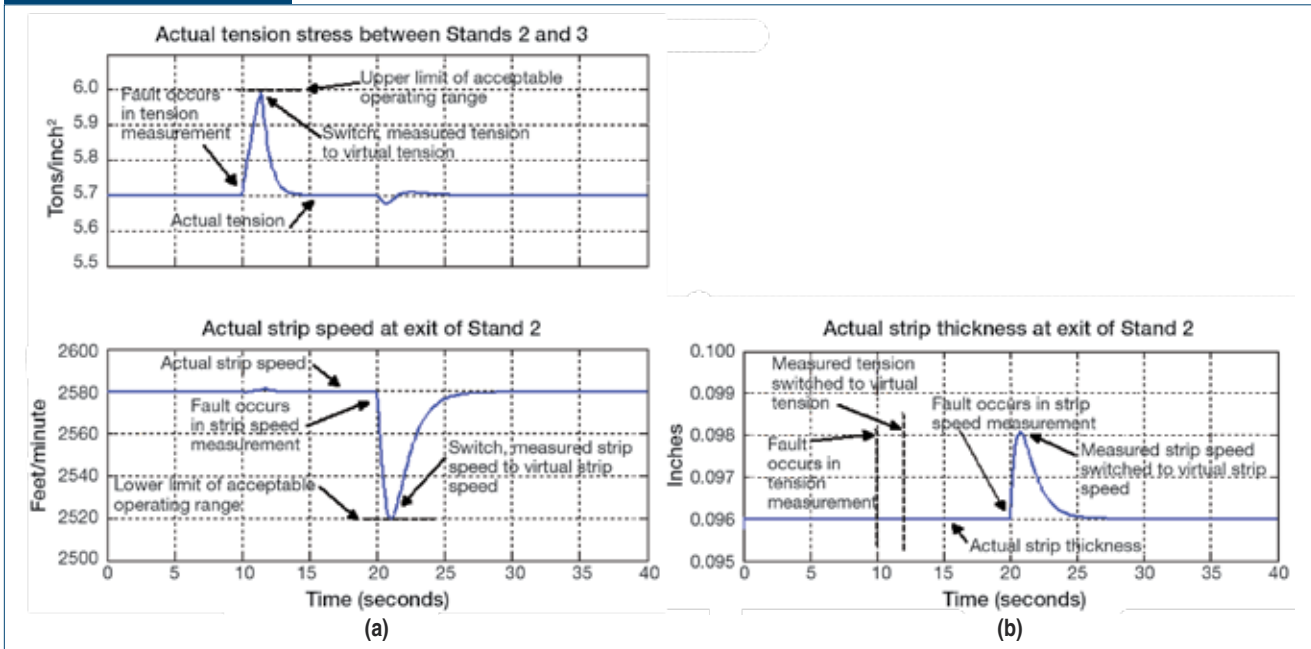
The simulations were done using MATLAB\Simulink. Initially, simulations were performed without uncertainties to verify the main concepts of the control technique. In these simulations, faults in the tension measurement and the strip speed measurement were addressed. The results are depicted in Figs. 4 and 5.

In Figs. 4b and 5b, the excursion in the actual strip thickness for the fault in the tension measurement is negligible with respect to the excursion in the thickness for the fault in the strip speed measurement. It also can be noted that excursions in the tension during a fault in the strip speed measurement are minor, and similarly in the strip speed for a fault in the tension measurement. As can be seen in Figs. 4 and 5, a fault in either the increasing or the decreasing direction is successfully handled by the controller. In all cases, the magnitude of the peak excursion in the actual strip thickness is about 2%, so that excursions in both actual thickness and tension are quite low, which contributes well to the overall quality of the end product. This good performance is retained irrespective of whether the tension or strip speed is actual or virtual.

Simulations were done to evaluate performance in the presence of uncertainties with typical results as noted in the example of Fig. 6.

In the case of the tension as shown in Fig. 6a, a simulation was started with an uncertainty of  $-2\%$  in the measured tension, with the actual tension at  $+2\%$  due to closed-loop control action, and with an uncertainty of  $+5\%$  in the virtual tension. A fault in the measured tension was initiated at 20 seconds. The fault was simulated such that the gain in the tension measurement began to decrease, which, due to closed-loop control action, caused the actual tension to increase to hold the tension feedback at the reference tension. The virtual tension then followed the actual tension with an uncertainty of  $+5\%$ . The fault is detected when the virtual tension exceeds 10% of the desired tension; the switch to the virtual tension then is made, so that the tension feedback is now the

Figure 4

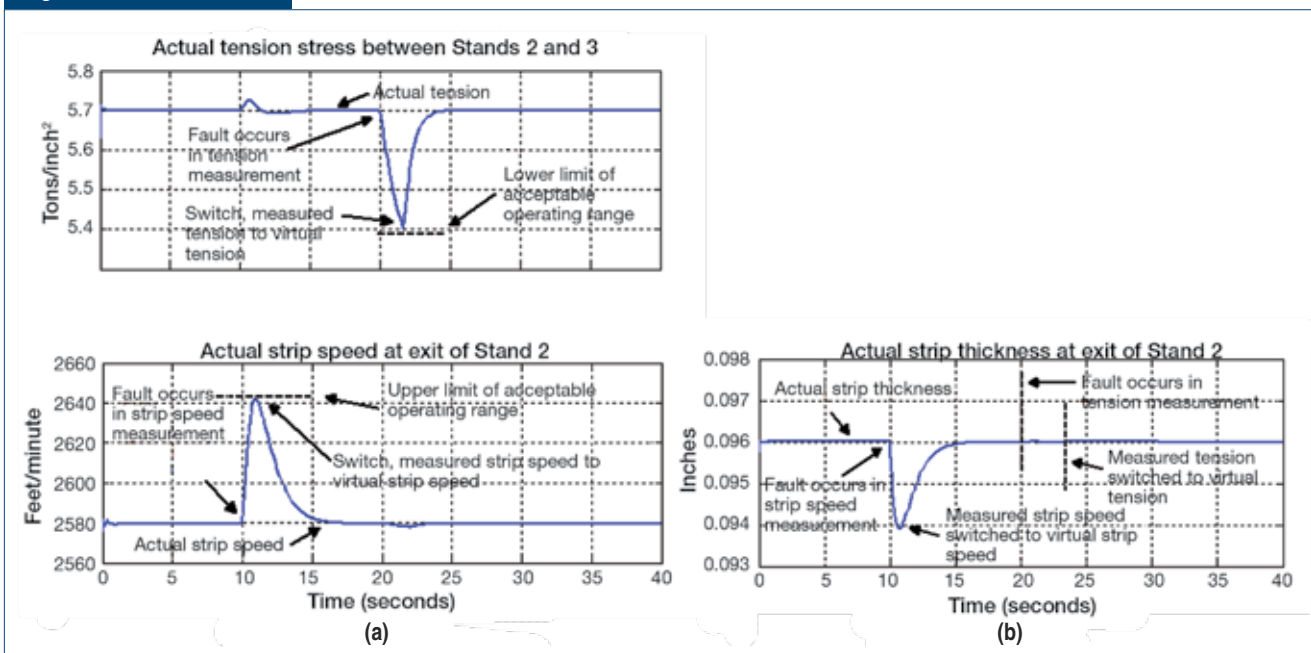


Responses for faults in tension and strip speed measurements (a), and strip thickness response (b), without uncertainties.

virtual tension, which is 5% above the actual tension. The steady-state actual tension then becomes -5% of the desired tension since the virtual tension is the feedback to the controller and therefore is held at the reference tension.

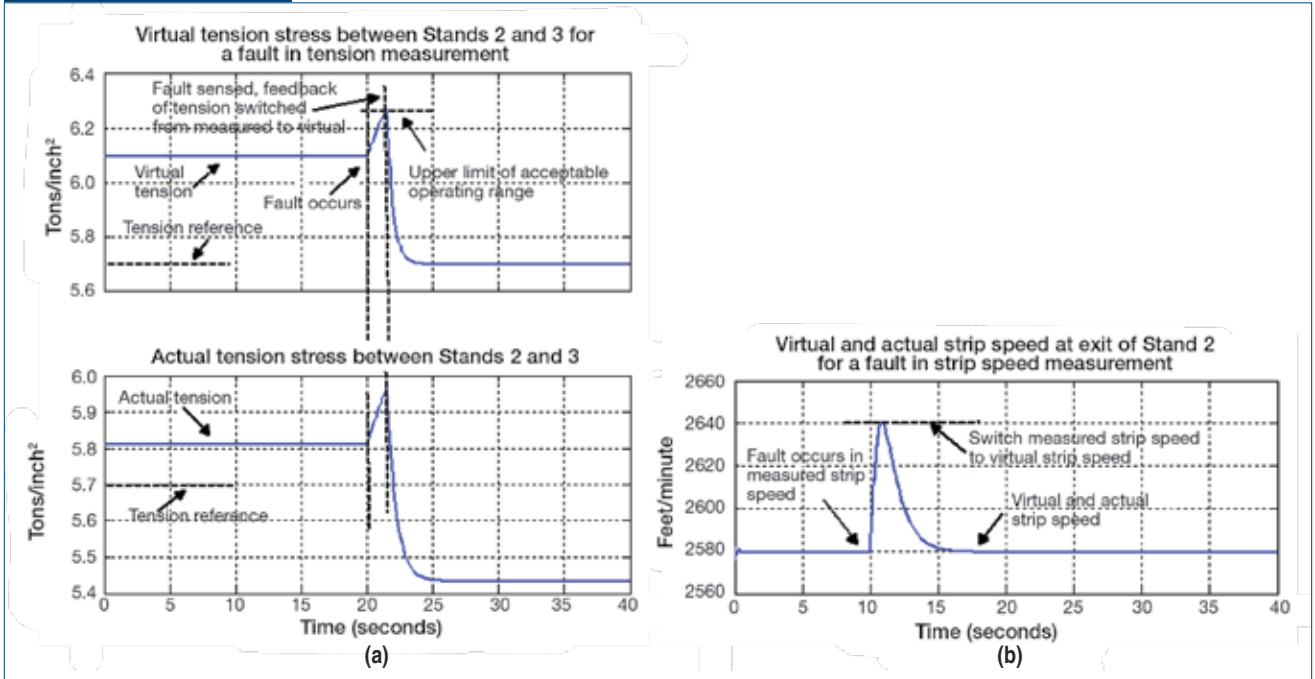
In the case of the strip speed measurement as shown in Fig. 6b, the measured speed has negligible uncertainty so that, prior to the fault, the actual speed and the virtual speed are very nearly the same as the measured speed. This is because the virtual speed has

Figure 5



Responses for faults in tension and strip speed measurements (a), and strip thickness response (b), without uncertainties, and with positions and fault directions inverted from what is depicted in Fig. 4.

Figure 6



Responses for a fault in tension measurement (a), and in strip speed measurement with uncertainties (b).

been calibrated to be very nearly the actual speed as described previously, and with the uncertainty in the measured speed being essentially zero. After the fault occurs, the measured speed is no longer very nearly the actual speed, but with the measured speed still being used in the determining of the strip thickness (Eq. 23). The fault in the measured speed is indicated by the separate speed measurement system. Upon detection of the fault, the speed measuring system issues a signal that is used in the controller to switch to the virtual speed. In the event of the failure of the speed measurement system to detect the fault, a backup function in the controller uses successive changes in  $k_2$  (Eq. 24) to detect an eventual out-of-range calibration and switch to the virtual, but with a higher uncertainty in the virtual speed. In the event that the fault occurs during the scan of the controller for the calibration of the virtual speed, the calibration function will be blocked by logic in the controller, so that the previous calibration is used, but with a slightly larger uncertainty. However, this event is extremely unlikely, and even if it does occur, the fault is detected and the switch to the virtual speed is made.

## Conclusions

The preceding simulations have confirmed the capability of the methodology described herein to successfully handle faults in certain measurements. This

technique can be applied also to other measurements to ensure continuance of operation in the presence of faults in these measurements. In addition, it can be a basis for further work to investigate the potential for reduction in the number of sensors, and to realize significant improvements in the availability of other industrial processes.

## Appendix

**Responses to Various Types of Faults** — Generally, it is recognized in the applicable literature that most faults are of two types:<sup>7,8</sup> (1) Faults that are failures of functions that fail and remained failed, and (2) Faults that are malfunctions that can drift into and out of failed conditions. In the methodology as presented previously, the system is capable of handling both of these situations. In either case, the initial detection of a faulted condition will actuate a short time delay before a valid fault is declared by the switching logic. This avoids the false declaration of a fault wherein a very short malfunction in the monitored function might exceed the acceptable operating level during normal operation of the controller. Additionally, suitable logic is included so that a series of closely repeated, very short malfunctions are recognized as a valid fault, even though the time delay function is not actuated to declare a fault at each malfunction. The detailed characteristics of the time delay function and

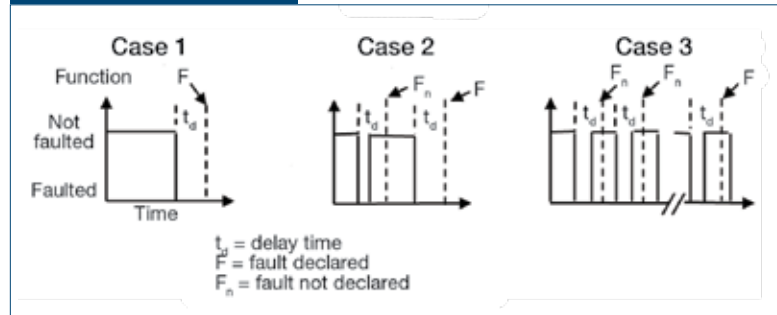
associated logic are set by the designer based on the requirements of the actual application. Appendix 1 presents three example cases.

In Case 1, the function being monitored has failed and remains failed; after a time delay, a fault is declared. In Case 2, a malfunction of short duration occurs, but no fault is declared since the function has recovered when the time delay has expired. The malfunction then reoccurs and remains after the time delay has expired so that a fault is declared. In Case 3, a series of malfunctions of short duration has occurred, but no fault is declared until the logic determines that the malfunction pattern has a good possibility of representing an actual fault. Thus, as these examples show, actual faults are declared and the likelihood of the declaration of false faults is reduced.

## References

1. J. Pittner and M.A. Simaan, *Tandem Cold Metal Rolling Control*, Springer-Verlag, London, U.K., 2011, Chapter 5.
2. J. Pittner and M.A. Simaan, "Improvement in the Tandem Rolling of Hot Metal Strip Using a New Advanced Control Technique," *Iron & Steel Technology*, Vol. 10, No. 12, December 2013, pp. 67–81.
3. J. Pittner and M.A. Simaan, *Tandem Cold Metal Rolling Control*, Springer-Verlag, London, U.K., 2011, Chapter 2.
4. J.G. Lenard, M. Pietrzyk and L. Cser, *Mathematical and Physical Simulation of Hot Rolled Products*, Elsevier, Amsterdam, 1999, p. 91.
5. H. Ford, E.F. Ellis and D.R. Bland, "Cold Rolling With Strip Tension, Part I-A New Approximate Method of Calculation and Comparison With Other Methods," *Journal of the Iron and Steel Institute*, Vol. 168, May 1951, pp. 57–72.
6. T. Cimen, "Systematic and Effective Design of Non-Linear Feedback Controllers Via the State-Dependent Riccati (SDRE) Method," *Annual Reviews in Control*, Elsevier, 34, 2010, pp. 32–51.
7. R. Isermann, *Fault Diagnosis Applications*, Springer-Verlag, Heidelberg, Germany, 2011, Chapter 2.
8. E. Sobhani-Tehrani and K. Khorasani, "Fault Diagnosis of Non-Linear Systems Using a Hybrid Approach," *Lecture Notes in Control and Information Sciences 383*, Springer-Verlag, New York, N.Y., USA, 2009, Chapter 1. ◆

## Appendix 1



Example cases of fault declarations

This paper was presented at AISTech 2018 — The Iron & Steel Technology Conference and Exposition, Philadelphia, Pa., USA, and published in the Conference Proceedings.